Qi Li[1,2], Qing Sun[3], Manman Xie[3], Yuan Ling[4], Zeyang Zhu[1], Qingzeng Zhu[1], Nan Zhan[3], Guoqiang Chu[1,5,6]

[1]Institute of Geology and Geophysics, Chinese Academy of Sciences, Beijing 100029, China.

[2] University of Chinese Academy of Sciences, Beijing 100049, China.

[3] National Research Center of Geoanalysis, Beijing 100037, China.

[4] Institute of Geology, Chinese Academy of Geological Sciences, Beijing 100037, China.

[5] CAS Center for Excellence in Life and Paleoenvironment, Beijing 100044, China.

[6] Innovation Academy for Earth Science, Chinese Academy of Sciences, Beijing 100029, China.

Corresponding author:

G. Chu (chuguoqiang@mail.igcas.ac.cn) and Q. Sun (sunqing1616@yahoo.com)

Key Points:

- A temperature record over last 20 ka from Huguangyan Maar Lake in tropical China based on brGDGTs
- The Holocene temperature evolution at Huguangyan Maar Lake characterized with a regional-scale temperature change
- Ice volume may be main driving force on the temperature change of Huguangyan Maar Lake region from the Last Glacial Maximum to Holocene

Abstract

Discrepancies exist in global temperature evolution from the Last Glacial Maximum to the present between model simulations and proxy reconstruction. This debate is critical for understanding and evaluating current global warming on a longer timescale. Here we report a branched GDGTs-based temperature reconstruction from the sediments of Huguangyan Maar Lake in southeast China and validate it using historical documentary evidence and instrumental data. The reconstructed mean annual air temperature (MAAT) indicates distinct changes during the last deglaciation (Oldest Dryas, Bølling-Allerød, Younger Dryas). During the Holocene, temperatures gradually increased from the end of the Younger Dryas to ~7.0 ka BP, followed by a decrease in recent decades. However, our terrestrial temperature record differs with model simulations and proxy sea surface temperature records of the Holocene. We conclude that ice volume or ice sheet is the most prominent forcing that controlled the regional temperature evolution from the Last Glacial Maximum to the beginning of the middle Holocene; while the temperature variations during the middle and late

Holocene were mainly regulated by several possible factors, such as oceanic and atmospheric circulation, and external drivers (solar and volcanic activity).

1 Introduction

There is an ongoing debate about the Holocene temperature record of the extra-tropical Northern Hemisphere. Proxy records show a general long-term cooling trend since the early Holocene (Marcott et al., 2013), while model simulations indicate a warming trend over the past ~12,000 years (Liu et al., 2014). Models play an important role in understanding how climate systems respond to various forcing factors and boundary conditions. However, many dynamic processes are not well computed or weighted in the model simulations, such as external forcing factors (solar irradiance and explosive volcanism), and the internal variability of the climate system (e.g., ENSO, PDO, AO, and the monsoon). Moreover, proxy-based temperature reconstructions are often of low resolution and have relatively large uncertainties in proxy calibration and dating, as well as regional or seasonal biases. Hence, more regional proxy-based paleoclimate time series are needed to verify the climatic record of the Holocene and to understand the differences between model simulations and paleoclimate reconstructions.

In this study, we present a high resolution branched glycerol dialkyl glycerol tetraethers (brGDGTs) membrane lipids-based temperature reconstruction (0-10 ka BP) combined with previously published data (10-20 ka BP) from the sediments of Huguangyan Maar Lake (21°9´N, 110°17´E) in tropical China (Chu et al., 2017), with the aim of obtaining a regional terrestrial temperature record and to understand its dynamic links.

Our paleotemperature proxy is based on brGDGTs, which comprise two dialkyl chains with different amounts of methyl and cyclopentane moieties (Damsté et al., 2009; Hopmans et al., 2004; Naafs et al., 2017; Sanchi et al., 2014; Schouten et al., 2000; Schouten et al., 2013; Sun et al., 2011; Tierney & Russell, 2009; Weijers et al., 2007). The physical and biological mechanisms of the temperature sensitivity of brGDGTs could be due to their membrane components maintaining membrane fluidity via methyl and cyclopentane moieties (Damsté et al., 2002; Huguet et al., 2007; Weijers et al., 2007). The methylation index of branched tetraethers (MBT) and the cyclization ratio of branched tetraethers (CBT) have previously been used to reconstruct terrestrial paleotemperatures from lacustrine sediments, soils, and peat sequences (Ding et al., 2015; Naafs et al., 2017; Peterse et al., 2012; Weijers et al., 2007; Yang et al., 2014).

Numerous studies have confirmed that brGDGTs-based indices from lacustrine sediments can be used to reconstruct terrestrial paleotemperatures (De Jonge et al., 2014; Hu et al., 2016; Kaiser et al., 2015; Loomis et al., 2012; Martin et al., 2020; Naafs et al., 2017; Pearson et al., 2011; Russell et al., 2018; Sun et al., 2011; Tian et al., 2019; Tierney et al., 2010; Weijers et al., 2007; Zink et al., 2016). However, several interpretational uncertainties remain, such as regarding the relative contributions of aquatic sources and soil sources to brGDGTs because the calibration functions from soils and lakes are quite different. Huguangyan

Lake is a small, hydrologically-closed lake with no inflows and a small watershed area, and therefore the sedimentary organic matter originates mainly in the water column (Chu et al., 2017; Hu et al., 2016). The within-lake origin of the sedimentary organic matter, which is also supported by the relatively low sedimentary TOC/N ratios since ~20 ka BP (Chu et al., 2002), substantially reduces this source of uncertainty in paleotemperature reconstruction. Previous brGDGTs-based MAAT reconstructions during the last deglaciation from the sediments of Huguangyan Maar Lake demonstrated a distinctive pattern of temperature changes from during the Oldest Dryas, Bølling-Allerød, Younger Dryas, and the onset of the Holocene (Chu et al., 2017).

2 Materials and Methods

2.1 Study site

Maar lakes are recognized as ideal sites for preserving high-resolution sedimentary archives because they are closed basins with a relatively simple hydrological system and they provide continuous sedimentary sequences (Yancheva et al., 2007). Huguangyan Maar Lake is a closed basin without stream inputs located in the Leizhou Peninsula in the tropical region of South China. The surface area is 2.3 km2, the maximum water depth is 22 m, and the watershed area is 3.2 km2 (Figure 1) (Chu et al., 2002; Yancheva et al., 2007). The area has a mean annual air temperature of 23.4℃ and a temperature difference between winter and summer of 11.9℃ (1964–2004; data from Zhanjiang meteorological station). Overlapping piston cores were collected from near the center of the lake in a water depth of 14 m. The cores were sliced at a 1-cm interval and then freeze dried for GDGTs extraction.

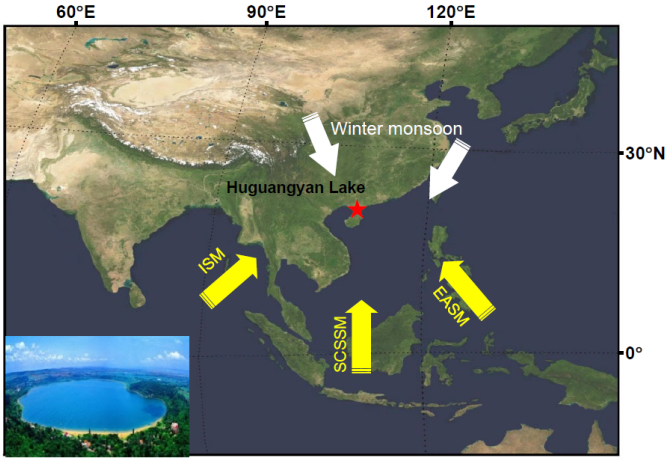

Figure 1. Location of Huguangyan Maar Lake. Solid arrows indicate the dominant direction of the summer monsoon (yellow) and winter monsoon (white). The inset photo shows Huguangyan Lake. Background image is modified from NASA (http://visibleearth.nasa.gov).

2.2 Chronology

The sedimentary chronology for Huguangyan Maar Lake is based on 14 AMS ^{14}C dates from handpicked leaves and/or other terrestrial plant macrofossils, together with analyses of ^{137}Cs and ^{210}Pb concentrations (Table 1; Figure 2; Supplementary Figure S1). The results of radiometric dating (^{137}Cs, ^{210}Pb, AMS^{14}C) have been presented previously (Chu et al., 2017; Wang et al., 2016).

Table 1. Radiocarbon ages from Huguangyan Maar Lake.

Lab. code	**Material**	**Depth (cm)**	**Radiocarbon age (BP)**	**Calibrated age (Median)**
Poz-47119	Leaves	53	850±40	738
Poz-47120	Leaves	94	1200±50	1135
Poz-47121	Branch	135	1275±30	1233
Poz-47122	Leaves	179	1875±35	1822
Poz-47187	Leaves	290	3650±35	3941
Poz-47123	Leaves	399	4140±40	4644
Poz-47124	Leaves	541	6280±40	7215
Poz-47188	Leaves	626	9420±80	10640
Poz-47125	Leaves	671	10300±70	12246
Poz-47127	Leaves	731	11430±60	13427
Poz-47128	Leaves	815	13420±70	16122
Poz-47129	Charcoal	882	14530±170	17399
Poz-47130	Charcoal	936	15590±120	18619
Poz-47131	Charcoal	1026	16980±200	20219

All AMS ^{14}C ages were calibrated using the atmospheric data set from the calibration program CALIB 4.3 (Stuiver et al., 1998).

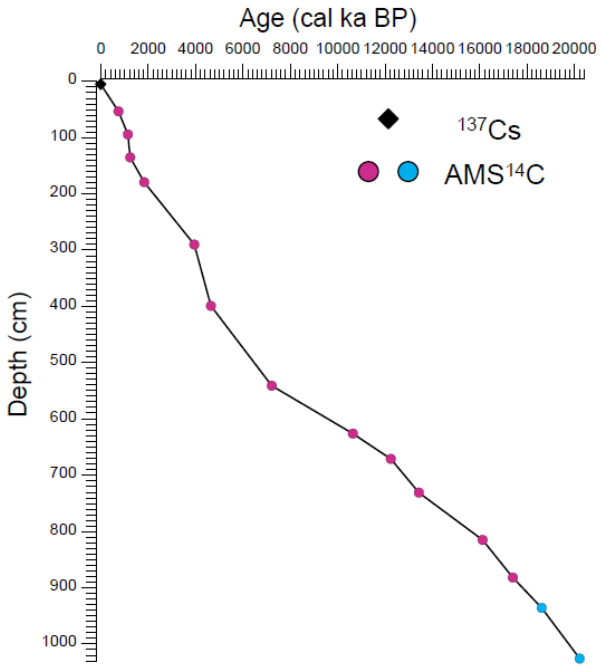

Figure 2. Age-depth plot for the Maar Lake Huguangyan. The calibrated AMS14C dates are from Wang et al., (2016) (red) and Chu et al., (2017) (blue).

2.3 GDGTs analysis

This study builds upon previous work of Huguangyan Maar Lake (Chu et al., 2017). For GDGTs analysis, freeze-dried samples (~1.5 g) were extracted using a dichloromethane (DCM): methanol (9:1, v/v) mixture with an accelerated solvent extractor (ASE 350) at 120 ℃ and 1500 psi for two cycles. The extracts were dried under N_2 and separated into apolar and polar fractions over an activated Al2O3 column using hexane: DCM (9:1, v/v) and DCM: methanol (1:1, v/v) as the respective eluents.

The branched GDGTs were analyzed using a Shimadzu high-performance liquid chromatography triple quadrupole mass spectrometry system (HPLC-MS), with an autosampler and Analyst software (modified by Hopmans et al., 2004; Weijers et al., 2007). Separation was achieved using a Grace Prevail Cyano column (150 mm × 2.1 mm; 3 m); ion scanning was performed in a single ion monitoring mode at m/z 1050, 1048, 1046, 1036, 1034, 1032, 1022, 1020 and 1018. The brGDGTs were quantified using a C46 internal standard.

MAAT from brGDGT for the Huguangyan Maar Lake was obtained using the degree of methylation (MBT) and the cyclisation ration of branched tetraether (CBT) according to the proxy calibration for the lacustrine sediment from China and Nepal (Sun et al., 2011):

MAAT=3.949 – 5.593 × CBT + 38.213 × MBT (n=100, r^2=0.73)

3 Result and Discussion

3.1 Reconstruction temperature vs. instrumental data and historical documentary.

All proxy data are indirect measurements of climate change, and therefore it is necessary to calibrate or validate them against instrumental or other independent data(Jones & Mann, 2004). Hence, we compared the brGDGTs-based MAAT record from Huguangyan Maar Lake with several other independent climate datasets: instrumental annual mean air temperature data from Zhanjiang meteorological station, ~15 km from Huguangyan Lake; historical documents from 140 local chronicles and 14 monographs from southern China (south of 23.5ºN), and a synthetic temperature reconstruction for China (Figure 3c).

The reconstructed MAAT is 22.5℃ for the period of 2010 CE–1951 CE (based on 137Cs-dating of the uppermost part of the sediment column). This result is close to the instrumental annual mean air temperature (23.2℃) for the same period obtained from nearby Zhanjiang meteorological station, however, there is a 0.7℃ offset between the instrumental data and the reconstructed temperatures. Although temperatures in this tropical lake are favorable for biological activity throughout the year, the brGDGTs-based temperature is slightly biased to winter and spring temperatures because of the turnover of the water column, which causes nutrient-rich bottom water to reach the surface and support the growth of aquatic organisms. This was confirmed by the seasonal flux of brGDGTs estimated from sediment traps (Hu et al., 2016), together with monthly observations of planktonic diatoms (Wang et al., 2012). The occurrence of lower temperatures during the 1970s is confirmed by both instrumental data for 1921 CE–1939 CE and 1951 CE–2010 CE, as well as by the MAAT reconstruction (Figure 3a).

Historical documents have often been used for paleoclimatic reconstruction. In tropical China, historical documents are widely available and there are hundreds of local chronicles. Direct descriptions using terms such as “rivers frozen” and “snow, sleet and frost” in tropical China (south of 23º30’ N) are interpreted as clear evidence of cold events. These abnormal phenomena are related to cold surges (cold waves). Meteorologically, a cold surge has been defined as a very large temperature decrease (exceeding 8℃) within 24 hours, and they are proposed as a surrogate for winter monsoon strength in China (Ray et al., 1991). Cold surges have a relatively short duration, often less than one week. We used historical documents to produce a compilation of evidence of “rivers frozen, snow, sleet and frost in the tropical plains” (south of 23.5º N; see Supplementary Table S1). The sources are from ”Natural disasters in historical documents in Guangdong province” (including Hainan province) and ”Natural disasters in historical documents in Guangxi province” (Institute of Literary and History, Guangdong Province, unpublished data), which consist of 140 local chronicles and 14 monographs.

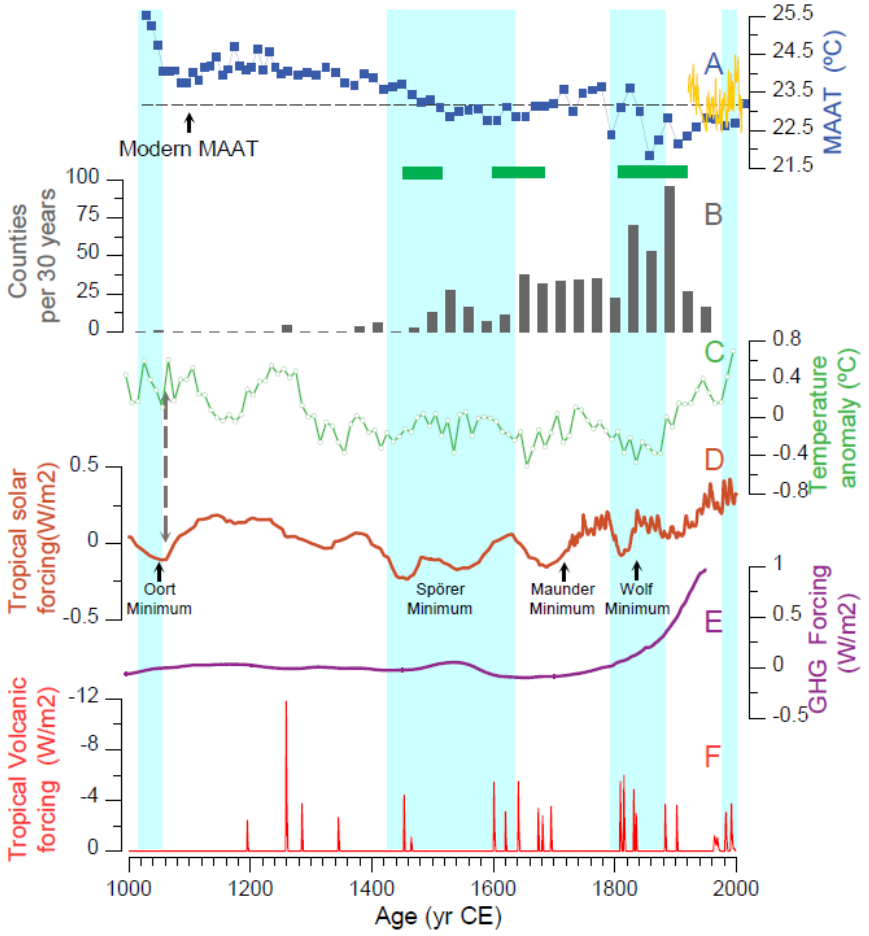

Figure 3. Comparison of the brGDGTs-based MAAT record for Huguangyan Maar Lake with historical documentary evidence, instrumental data, and possible climate forcings during the last millennium. (**a**) brGDGTs-based MAAT record obtained in this study (blue line); annual mean air temperature from Zhangjiang Station (1921–1939 and 1951–2010) (yellow line); modern MAAT for the study area (green dashed line). (**b**) Number of counties with cold surges per 30 years in tropical China years from historical documents; (**c**) Synthetic temperature reconstruction for China (Ge et al., 2015); (**d**) Record of tropical solar forcing (Mann et al., 2005); (**e**) record of GHG radiative forcing (CO_2, CH_4, N_2O) (Köhler et al., 2017); (**f**) Record of tropical volcanic forcing (Mann et al., 2005); Green bars represent the extreme cold winters based on historical documentary evidence from China (Chu and Ching, 1973).

Extreme cold events are concentrated in the Little Ice Age, especially between 800 CE and 1900 CE, while the Medieval Warm Period (MWP) had few fewer cold events (Figure 3b). Historical records are less abundant and intermittent

before 1400 CE but are more continuous after the Ming Dynasty (the Fang Zhi (local chronic) period of 1400 CE-1900 CE). The brGDGTs-based MAAT record from Huguangyan Maar Lake shows three cold intervals: 440 CE-1640 CE, 1800 CE-1890 CE, and during the 1970s (Figure 3a). Within the limits of the dating uncertainties, these intervals are consistent with the documentary evidence (Figure 3b).

Natural climate forcings such as changes in solar output and volcanic eruptions are widely recognized as causes of decadal-to-centennial–scale climatic variations. Figure 3 shows that most of the cold intervals recorded at Huguangyan Maar Lake correspond to sunspot minima and episodes of intensified volcanic activity. However, the decrease in MAAT at ~1740 CE is not linked to these forcings.

3.2 Holocene brGDGTs-based temperature change

Although the climate of the Holocene, the most recent interval of Earth history, was more stable than that during the last glacial period, it was interrupted by several abrupt cooling events on the decadal- to centennial-scale (Bond et al., 2001). The brGDGTs-based temperature record from Huguangyan Maar Lake shows an increase in MAAT from 22℃ after the Younger Dryas (11.5 ka BP) to 28℃ by ~7.0 ka BP, followed by a gradual decrease from 23.5℃ in recent decades. This general trend is punctuated by eight cooling events on the decadal-to centennial-scale, centered at 0.4, 2.0, 3.7, 5.3, 5.8, 8.3, 9.0, and 9.6 ka B.P. (Figure 4, 5).

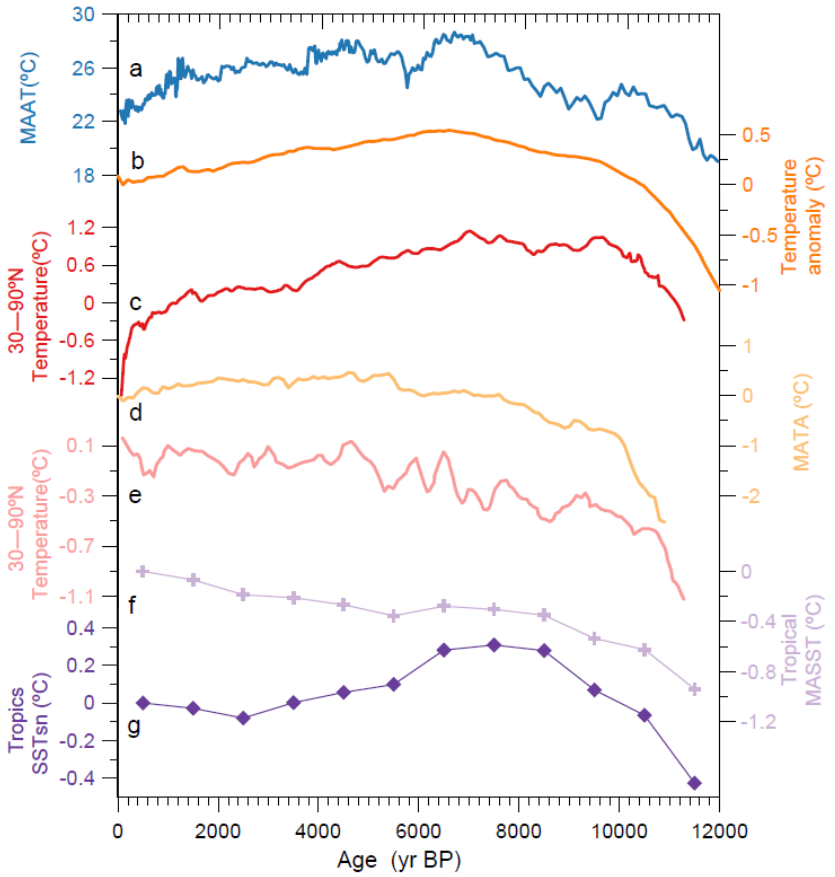

Figure 4. Comparison of the Holocene brGDGTs-based MAAT record with temperature reconstructions and model simulations. (**a**) BrGDGTs-based MAAT from Huguangyan Maar Lake (this study); (**b**) Global mean surface temperature (Temp12k; Kaufman et al., 2020); (**c**) Proxy-based mean temperature of the Northern Hemisphere (90º–30º N; Marcott et al., 2013); (**d**) Pollen-based mean annual temperature anomaly (MATA) for North America and Europe (Marsicek et al., 2018); (**e**) Model-based simulation of the temperature of the Northern Hemisphere (90º–30 ºN; Liu et al., 2014); (**f**) Seasonally-unadjusted SST record (SST_{SN}, 23.5º–23.5ºN; Bova et al., 2021); (**g**) Tropical mean annual SST record (MASST, 23.5ºS–23.5ºN; Bova et al., 2021).

Spectral analysis of the brGDGTs-based temperature series since 8.0 ka BP revealed several statistically significant quasi-periodicities, from the multi-decadal to the centennial scale: 201-202, 111-112, 95-96, 92-93, 78-82, and 64-65 years. Several of these periodicities are close to those of significant solar cycles, such as the Gleissberg cycle (~70–100 yr) and the de Vries cycle (~200-210 yr), although the latter is less significant in the time series (see Supplementary Figure S2).

The record from Maar Lake Huguangyan is indicative of regional-scale temperature change. A comparison of the record with subcontinental and hemispheric temperature time series is shown in Figure 4. In terms of general trends, the brGDGTs-based MAAT record shows a decreasing trend similar to that of global mean surface temperature (Temp12k; Kaufman et al., 2020), and proxy-based mean temperature in the Northern Hemisphere (90°-30°N; Marcott et al., 2013), but it is in conflict with model simulations of the temperature of the Northern Hemisphere (90°-30 °N; Liu et al., 2014) and of tropical mean annual sea surface temperature (MASST, 23.5°S-23.5°N; Bova et al., 2021). Thus, the Holocene temperature evolution at Huguangyan Maar Lake contrasts with the results of model simulations. One of the reasons for this may be the existence of a model simulation bias in SST reconstructions and uncertainty in the weighting of different forcings.

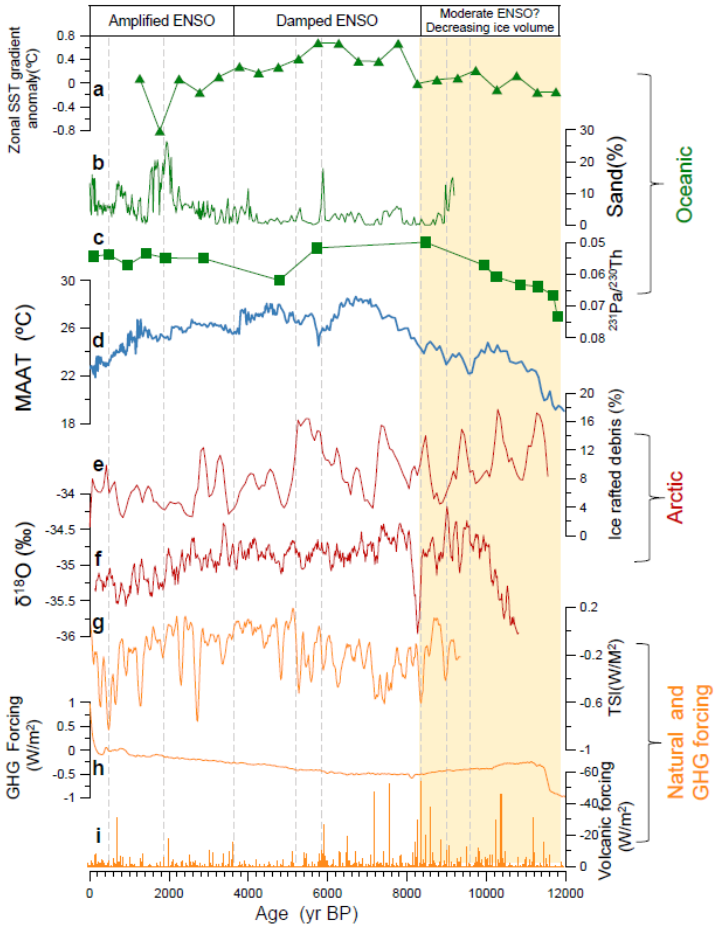

Figure 5. Comparison of the Holocene brGDGTs-based MAAT record from Huguangyan Maar Lake with potential independent internal and external drivers

of climate change. (**a**) Zonal SST gradient anomaly relative to the late Holocene calculated as the difference between the western and eastern Pacific (Koutavas and Joanides, 2012); (**b**) ENSO record from Lake El Junco in the Galápagos Islands (Conroy et al., 2008); (**c**) Sedimentary record of $^{231}Pa/^{230}Th$ from the subtropical North Atlantic Ocean (McManus et al., 2004); (**d**) brGDGTs-based MAAT record from Huguangyan Maar Lake (the data for 10–20 kyr BP are from Chu et al., 2017); (**e**) Ice rafted debris record from North Atlantic sediment cores (Bond et al., 2001); (**f**) Greenland ^{18}O ice core record (GRIP,11-point running average) (Vinther et al., 2006); (**g**) Record of total solar irradiance (TSI; Steinhilber et al., 2012); (**h**) Record of GHG radiative forcing (CO_2, CH_4, N_2O) (Köhler et al., 2017); (**i**) Record of Volcanic forcing from a Greenland ice core (Kobashi et al., 2017).

The MAAT at Huguangyan Maar Lake can potentially help understand the dynamical origin of both gradual and abrupt Holocene temperature changes. Widely accepted potential drivers of climate change include fluctuations of ice volume or ice sheet dynamics, external drivers such as solar and volcanic activity, ocean circulation (e.g., involving North Atlantic Deep Water, Antarctic Bottom Water, and ENSO), polar sea ice, and atmospheric greenhouse gases (GHG).

Our results suggest that ice volume or ice sheet dynamics suppressed any other forcings and controlled the regional temperature evolution from the last glacial maximum to the early Holocene (8.2 ka BP; Figure 4, 5). GHG radiative forcing (CO2, CH4, N2O; Köhler et al., 2017) may be a secondary factor. Several previous studies have highlighted the importance of ice-sheet dynamics as a driver of temperature change (Baker et al., 2017; Liu et al., 2014; Marsicek et al., 2018). For example, the ^{18}O record from Kinderlinskaya cave in the Ural Mountains, which is interpreted as a winter temperature proxy (Baker et al., 2017), reveals negative ^{18}O anomalies at 11.0 and 8.2 ka BP, which could be caused by the effects of enhanced meltwater influx from melting Northern Hemisphere ice sheets on North Atlantic Ocean circulation (Baker et al., 2017).

Changes in North Atlantic Deep Water (NADW), Atlantic Meridional Overturning Circulation (AMOC), and Antarctic Bottom Water (ABW) have been suggested as major causes of abrupt climate changes (McManus et al., 2004; Struve et al., 2020). Both the AMOC (McManus et al., 2004) and Antarctic Bottom Water (UCDW and AAIW) show a pronounced shift in the middle Holocene (Figure 5), and the distinct temperature shift at ~5.8 ka BP evident in the MAAT record from Huguangyan Maar Lake could be related to this major change in oceanic circulation.

El Niño–Southern Oscillation (ENSO) variability and the ENSO mode (e.g., EP, CP) may significantly influence both SSTs and temperature changes in some terrestrial regions. Generally, El Niño is significantly positively correlated with winter air temperature variability, especially in the case of the negative temperature anomalies in eastern China during the EP La Niña phase (Ren et al., 2020; Wang et al., 2017). An amplified ENSO in the late Holocene and a damped ENSO during the middle Holocene have also been recognized (Carré

et al., 2014; Conroy et al., 2008; Koutavas & Joanides, 2012), although their long-term linkage with climate in China is unclear.

Sea ice extent in the Arctic and Antarctic has been recognized as an important driver of abrupt climatic change on both interannual to annual timescales. The influence of sea ice on abrupt climatic events on decadal to centennial timescales via the amplification of sea-ice-albedo feedbacks, deep-water formation, and shifts of the Intertropical Convergence Zone (e.g., Bond et al., 2001; Moros et al., 2006) are also recognized. Bond et al. (2001) attributed abrupt Holocene climatic events recorded in marine sediment cores and other paleoclimatic records to the effects of changes in solar activity on sea ice extent via amplification and transmission processes involved in ocean-atmosphere circulation. However, the variation of sea-ice extent during the Holocene shows a complex pattern or even opposite trends in the Arctic oceans (Moros et al., 2006). Although it remains difficult to accurately reconstruct spatiotemporal changes in sea ice or ice-rafting (Moros et al., 2006), sea ice variability could be one of several important drivers of abrupt climate changes.

Within the limits of the dating uncertainty, most of the cooling events observed in the brGDGTs-based MAAT record can be linked to oceanic and external forcings; however, the effects of the solar minima at ~2.6, ~6.2 and ~7.4 ka BP are less clearly evident (Figure 5). The large temperature variations observed at tropical Huguangyan Maar Lake could also be caused by winter monsoon amplification. In continental Eurasia, the winter monsoon plays an important role in the amplification and rapid transmission of the temperature signal from the Arctic to the tropics, and in the migration of the intertropical convergence zone(Chu et al., 2017).

3.3 The brGDGTs-based temperature change during the last deglaciation

Previous brGDGTs-based records indicate that the average MAAT was 17.8ºC during the Oldest Dryas, which was followed by a gradual rise during the Bølling-Allerød interstadial, when it reached a maximum of 21.8℃ at 13.0 ka BP. Subsequently, the average MAAT decreased to 19.5℃ during the Younger Dryas (Figure 6b; Chu et al., 2017). This temperature pattern strongly suggests the influence of ice volume or ice sheet and meltwater dynamics on the temperature evolution of the Huguangyan Lake region from the Last Glacial Maximum to the early Holocene (Figure 6).

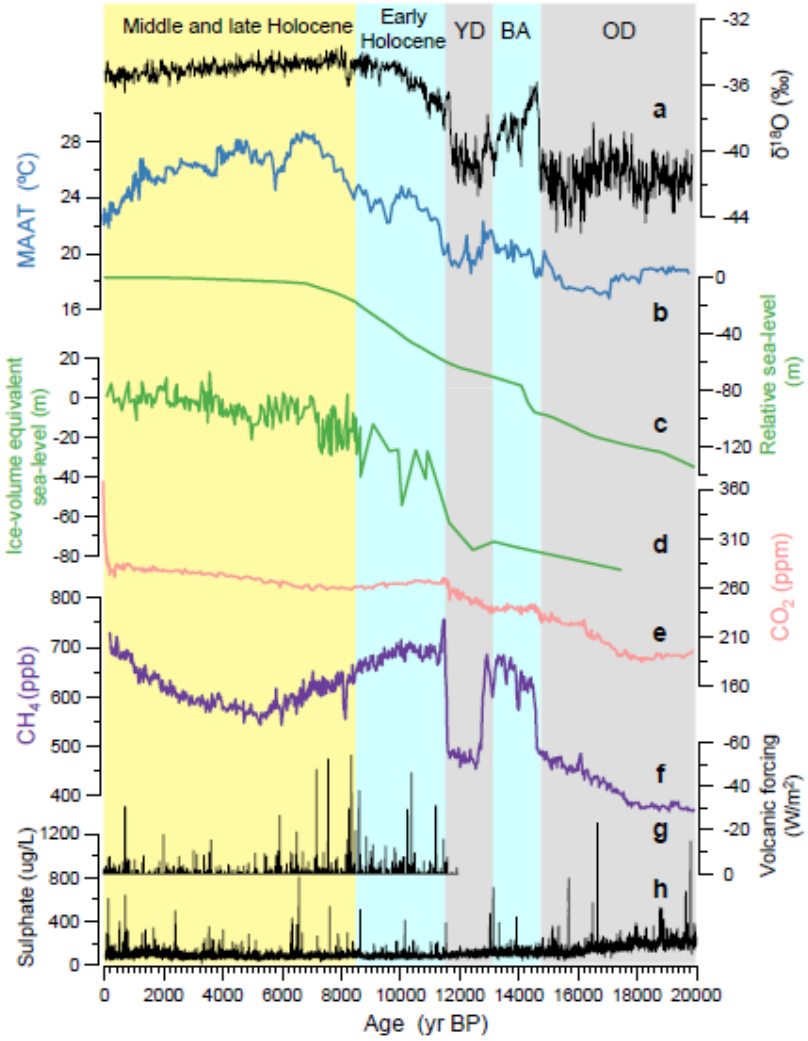

Figure 6. Comparison of the bGDGTs-based MAAT record (this study) with records of ice-volume equivalent sea-level and external climate forcings. (**a**) Greenland ^{18}O ice core (GRIP) record (Vinther et al., 2006); (**b**) bGDGTs-based MAAT record from Huguangyan Maar Lake (this study; The data for 10–20 kyr BP is from Chu et al., 2017); (**c**) Global ice volume record (relative sea level) from Grant et al. (2012); (**d**) Ice-volume equivalent sea-level record (Lambeck et al., 2014); (**e**) Dome C, antarctica, ice core CO_2 record (Bereiter et al., 2015); (**f**) WAIS Divide CH_4 concentration (Fudge et al., 2013); (**g**) Sulfate record of volcanic forcing from a Greenland ice core (Kobashi et al., 2017); (**h**) Sulfate record from the Dome C ice core, Antarctica (Castellano et al., 2004).

The most striking cooling events evident in the brGDGTs-based MAAT record

are linked with the abrupt weakening of the tropical summer monsoon (see Supplementary Figure S3). For example, the high-resolution ^{18}O record from Klang Cave in the Thai-Malay Peninsula (Chawchai et al., 2021) shows a large increase of 1.5 ‰ from 6.4 to 5.8 ka BP; and the $^{13}C_{27\text{-}35}$ record of leaf wax lipids from the annually laminated sediments of Myanmar Maar Lake Twintaung indicates abrupt failures of the tropical monsoon at ~3.8 and ~5.8 ka BP (Chu et al., 2020).

4 Conclusions

Our brGDGTs-based temperature record shows an increasing MAAT during the last deglaciation and early Holocene and reached a maximum at ~6.6 kyr BP, followed by a decrease in middle and late Holocene. It is noted that our temperature reconstruction is in good agreement with instrumental temperature from 2010 CE to 1951 CE. We contend that the last deglaciation and early Holocene temperature variation is linked with the ice volume and/or ice sheet, while the temperature variations during the middle and late Holocene could be ascribed to several possible factors, such as oceanic and atmospheric circulation, and external drivers in Huguangyan Lake region.

Author contributions

Funding acquisition: G. Q. Chu, Q. Sun

Investigation: G. Q. Chu, Z. Y. Zhu, Q. Z. Zhu

Methodology: Q. Li, M. M. Xie, N. Zhan ,Y. Ling

Writing-Original draft: Q. Li, G. Q. Chu, Q. Sun

Writing-reviewing & editing: Q. Li, G. Q. Chu, Q. Sun, M. M. Xie

Acknowledgments

This work was funded by the National Natural Science Foundation of China (Grant 42030507, 41877301), the National Key Research and Development Program of China (Grant 2017YFA0603400) and the Strategic Priority Research Program of the Chinese Academy of Sciences (Grant XDB26000000).

References

Baker, J.L., Lachniet, M.S., Chervyatsova, O., Asmerom, Y. & Polyak, V.J. (2017). Holocene warming in western continental Eurasia driven by glacial retreat and greenhouse forcing. Nature Geoscience, 10(6), 430-435. doi:10.1038/ngeo2953.

Bereiter, B., Eggleston, S., Schmitt, J., Nehrbass-Ahles, C., Stocker, T.F., Fischer, H., et al. (2015). Revision of the EPICA Dome C CO2 record from 800 to 600 kyr before present. Geophysical Research Letters, 42(2), 542-549. doi:10.1002/2014GL061957.

Bond, G., Kromer, B., Beer, J., Muscheler, R., Evans, M.N., Showers, W., et al. (2001). Persistent solar influence on north Atlantic climate during the Holocene.

Science, 294(5549), 2130-2136. doi:10.1126/science.1065680.

Bova, S., Rosenthal, Y., Liu, Z., Godad, S.P. & Yan, M. (2021). Seasonal origin of the thermal maxima at the Holocene and the last interglacial. Nature, 589(7843), 548-553. doi:10.1038/s41586-020-03155-x.

Carré, M., Sachs Julian, P., Purca, S., Schauer Andrew, J., Braconnot, P., Falcón Rommel, A., et al. (2014). Holocene history of ENSO variance and asymmetry in the eastern tropical Pacific. Science, 345(6200), 1045-1048. doi:10.1126/science.1252220.

Castellano, E., Becagli, S., Jouzel, J., Migliori, A., Severi, M., Steffensen, J.P., et al. (2004). Volcanic eruption frequency over the last 45 ky as recorded in Epica-Dome C ice core (East Antarctica) and its relationship with climatic changes. Global and Planetary Change, 42(1), 195-205. doi:10.1016/j.gloplacha.2003.11.007.

Chawchai, S., Tan, L., Löwemark, L., Wang, H.-C., Yu, T.-L., Chung, Y.-C., et al. (2021). Hydroclimate variability of central Indo-Pacific region during the Holocene. Quaternary Science Reviews, 253, 106779. doi:10.1016/j.quascirev.2020.106779.

Chu, G., Liu, J., Sun, Q., Lu, H., Wang, W. & Liu, T. (2002). The 'Mediaeval Warm Period' drought recorded in Lake Huguangyan, tropical South China. Holocene, 12, 511-516. doi:10.1191/0959683602hl566ft.

Chu, G., Sun, Q., Zhu, Q., Shan, Y., Shang, W., Ling, Y., et al. (2017). The role of the Asian winter monsoon in the rapid propagation of abrupt climate changes during the last deglaciation. Quaternary Science Reviews, 177, 120-129. doi:10.1016/j.quascirev.2017.10.014.

Chu, G., Zhu, Q., Sun, Q., Su, Y., Xie, M., Zaw, T. & Sein, K. (2020). Drought Cycles Over the Last 8,200 Years Recorded in Maar Lake Twintaung, Myanmar. Journal of Geophysical Research: Atmospheres, 125(9). doi:10.1029/2019jd032225.

Chu, K.S. & Ching, C. (1973), A preliminary study on the climatic fluctuations during the last 5,000 years in China.

Conroy, J.L., Overpeck, J.T., Cole, J.E., Shanahan, T.M. & Steinitz-Kannan, M. (2008). Holocene changes in eastern tropical Pacific climate inferred from a Galápagos lake sediment record. Quaternary Science Reviews, 27(11), 1166-1180. doi:10.1016/j.quascirev.2008.02.015.

Damsté, J.S.S., Ossebaar, J., Abbas, B., Schouten, S. & Verschuren, D. (2009). Fluxes and distribution of tetraether lipids in an equatorial African lake: Constraints on the application of the TEX86 palaeothermometer and BIT index in lacustrine settings. Geochim. Cosmochim. Acta, 73(14), 4232-4249. doi:10.1016/j.gca.2009.04.022.

Damsté, J.S.S., Schouten, S., Hopmans, E.C., van Duin, A.C.T. & Geenevasen,

J.A.J. (2002). Crenarchaeol. Journal of Lipid Research, 43(10), 1641-1651. doi:10.1194/jlr.M200148-JLR200.

De Jonge, C., Hopmans, E.C., Zell, C.I., Kim, J.-H., Schouten, S. & Sinninghe Damsté, J.S. (2014). Occurrence and abundance of 6-methyl branched glycerol dialkyl glycerol tetraethers in soils: Implications for palaeoclimate reconstruction. Geochim. Cosmochim. Acta, 141, 97-112. doi:10.1016/j.gca.2014.06.013.

Ding, S., Xu, Y., Wang, Y., He, Y., Hou, J., Chen, L. & He, J.S. (2015). Distribution of branched glycerol dialkyl glycerol tetraethers in surface soils of the Qinghai–Tibetan Plateau: implications of brGDGTs-based proxies in cold and dry regions. Biogeosciences, 12(11), 3141-3151. doi:10.5194/bg-12-3141-2015.

Dutt, S., Gupta, A.K., Clemens, S.C., Cheng, H., Singh, R.K., Kathayat, G. & Edwards, R.L. (2015). Abrupt changes in Indian summer monsoon strength during 33,800 to 5500 years B.P. Geophysical Research Letters, 42(13), 5526-5532. doi:10.1002/2015GL064015.

Fudge, T.J., Steig, E.J., Markle, B.R., Schoenemann, S.W., Ding, Q., Taylor, K.C., et al. (2013). Onset of deglacial warming in West Antarctica driven by local orbital forcing. Nature, 500(7463), 440-444. doi:10.1038/nature12376.

Ge, Q., Zheng, J. & Hao, Z. (2015). PAGES synthesis study on climate changes in Asia over the last 2000 years: Progresses and perspectives. Acta Geographica Sinica, 70(3), 355-363.

Grant, K.M., Rohling, E.J., Bar-Matthews, M., Ayalon, A., Medina-Elizalde, M., Ramsey, C.B., et al. (2012). Rapid coupling between ice volume and polar temperature over the past 150,000 years. Nature, 491(7426), 744-747. 10.1038/nature11593.

Gupta, A.K., Anderson, D.M. & Overpeck, J.T. (2003). Abrupt changes in the Asian southwest monsoon during the Holocene and their links to the North Atlantic Ocean. Nature, 421(6921), 354-357. doi:10.1038/nature01340.

Hopmans, E.C., Weijers, J.W.H., Schefuß, E., Herfort, L., Sinninghe Damsté, J.S. & Schouten, S. (2004). A novel proxy for terrestrial organic matter in sediments based on branched and isoprenoid tetraether lipids. Earth and Planetary Science Letters, 224(1), 107-116. doi:10.1016/j.epsl.2004.05.012.

Hu, J., Zhou, H., Peng, P.a. & Spiro, B. (2016). Seasonal variability in concentrations and fluxes of glycerol dialkyl glycerol tetraethers in Huguangyan Maar Lake, SE China: Implications for the applicability of the MBT–CBT paleotemperature proxy in lacustrine settings. Chemical Geology, 420, 200-212. doi:10.1016/j.chemgeo.2015.11.008.

Huguet, C., Smittenberg, R.H., Boer, W., Sinninghe Damsté, J.S. & Schouten, S. (2007). Twentieth century proxy records of temperature and soil organic matter input in the Drammensfjord, southern Norway. Organic Geochemistry, 38(11), 1838-1849. doi:10.1016/j.orggeochem.2007.06.015.

Jones, P.D. & Mann, M.E. (2004). Climate over past millennia. Reviews of Geophysics, 42(2). doi:10.1029/2003RG000143.

Kaiser, J., Schouten, S., Kilian, R., Arz, H.W., Lamy, F. & Sinninghe Damsté, J.S. (2015). Isoprenoid and branched GDGT-based proxies for surface sediments from marine, fjord and lake environments in Chile. Organic Geochemistry, 89-90, 117-127. doi:10.1016/j.orggeochem.2015.10.007.

Kaufman, D., McKay, N., Routson, C., Erb, M., Dätwyler, C., Sommer, P.S., et al. (2020). Holocene global mean surface temperature, a multi-method reconstruction approach. Scientific data, 7(1), 201. doi:10.1038/s41597-020-0530-7.

Kobashi, T., Menviel, L., Jeltsch-Thömmes, A., Vinther, B.M., Box, J.E., Muscheler, R., et al. (2017). Volcanic influence on centennial to millennial Holocene Greenland temperature change. Scientific Reports, 7(1), 1441. doi:10.1038/s41598-017-01451-7.

Köhler, P., Nehrbass-Ahles, C., Schmitt, J., Stocker, T.F. & Fischer, H. (2017). A 156 kyr smoothed history of the atmospheric greenhouse gases CO2, CH4, and N2O and their radiative forcing. Earth Syst. Sci. Data, 9(1), 363-387. doi:10.5194/essd-9-363-2017.

Koutavas, A. & Joanides, S. (2012). El Niño–Southern Oscillation extrema in the Holocene and Last Glacial Maximum. Paleoceanography, 27(4). doi:10.1029/2012PA002378.

Lambeck, K., Rouby, H., Purcell, A., Sun, Y. & Sambridge, M. (2014). Sea level and global ice volumes from the Last Glacial Maximum to the Holocene. Proceedings of the National Academy of Sciences, 111(43), 15296. doi:10.1073/pnas.1411762111.

Liu, Z., Zhu, J., Rosenthal, Y., Zhang, X., Otto-Bliesner, B.L., Timmermann, A., et al. (2014). The Holocene temperature conundrum. Proc Natl Acad Sci USA, 111(34), E3501-3505. doi:10.1073/pnas.1407229111.

Loomis, S.E., Russell, J.M., Ladd, B., Street-Perrott, F.A. & Sinninghe Damsté, J.S. (2012). Calibration and application of the branched GDGT temperature proxy on East African lake sediments. Earth and Planetary Science Letters, 357-358, 277-288. doi:10.1016/j.epsl.2012.09.031.

Mann, M.E., Cane, M.A., Zebiak, S.E. & Clement, A. (2005). Volcanic and Solar Forcing of the Tropical Pacific over the Past 1000 Years. Journal of Climate, 18(3), 447-456. 10.1175/JCLI-3276.1.

Marcott, S.A., Shakun, J.D., Clark, P.U. & Mix, A.C. (2013). A Reconstruction of Regional and Global Temperature for the Past 11,300 Years. Science, 339(6124), 1198-1201. doi:10.1126/science.1228026.

Marsicek, J., Shuman, B.N., Bartlein, P.J., Shafer, S.L. & Brewer, S. (2018). Reconciling divergent trends and millennial variations in Holocene temperatures. Nature, 554(7690), 92-96. 10.1038/nature25464.

Martin, C., Ménot, G., Thouveny, N., Peyron, O., Andrieu-Ponel, V., Montade, V., et al. (2020). Early Holocene Thermal Maximum recorded by branched tetraethers and pollen in Western Europe (Massif Central, France). Quaternary Science Reviews, 228. doi:10.1016/j.quascirev.2019.106109.

McManus, J.F., Francois, R., Gherardi, J.M., Keigwin, L.D. & Brown-Leger, S. (2004). Collapse and rapid resumption of Atlantic meridional circulation linked to deglacial climate changes. Nature, 428(6985), 834-837. 10.1038/nature02494.

Moros, M., Andrews, J.T., Eberl, D.D. & Jansen, E. (2006). Holocene history of drift ice in the northern North Atlantic: Evidence for different spatial and temporal modes. Paleoceanography, 21(2). doi:10.1029/2005PA001214.

Naafs, B.D.A., Inglis, G.N., Zheng, Y., Amesbury, M.J., Biester, H., Bindler, R., et al. (2017). Introducing global peat-specific temperature and pH calibrations based on brGDGT bacterial lipids. Geochim. Cosmochim. Acta, 208, 285-301. doi:10.1016/j.gca.2017.01.038.

Pearson, E.J., Juggins, S., Talbot, H.M., Weckström, J., Rosén, P., Ryves, D.B., et al. (2011). A lacustrine GDGT-temperature calibration from the Scandinavian Arctic to Antarctic: Renewed potential for the application of GDGT-paleothermometry in lakes. Geochim. Cosmochim. Acta, 75(20), 6225-6238. doi:10.1016/j.gca.2011.07.042.

Peterse, F., van der Meer, J., Schouten, S., Weijers, J.W.H., Fierer, N., Jackson, R.B., et al. (2012). Revised calibration of the MBT–CBT paleotemperature proxy based on branched tetraether membrane lipids in surface soils. Geochim. Cosmochim. Acta, 96, 215-229. doi:10.1016/j.gca.2012.08.011.

Ray, T.C., Daniel, P.R., Huey, T.L., Lev, S.S. & Winston, H. (1991), Indium tin oxide single-mode waveguide modulator, paper presented at Proc.SPIE.

Ren, M., Zhang, W., Geng, X. & Liu, C. (2020). ENSO impact on the variability of wintertime synoptic-scale air temperature over China and possible mechanisms behind. Acta Meteorologica Sinica, 78(2), 199-209.

Russell, J.M., Hopmans, E.C., Loomis, S.E., Liang, J. & Sinninghe Damsté, J.S. (2018). Distributions of 5- and 6-methyl branched glycerol dialkyl glycerol tetraethers (brGDGTs) in East African lake sediment: Effects of temperature, pH, and new lacustrine paleotemperature calibrations. Organic Geochemistry, 117, 56-69. doi:10.1016/j.orggeochem.2017.12.003.

Sanchi, L., Ménot, G. & Bard, E. (2014). Insights into continental temperatures in the northwestern Black Sea area during the Last Glacial period using branched tetraether lipids. Quaternary Science Reviews, 84, 98-108. doi:10.1016/j.quascirev.2013.11.013.

Schouten, S., Hopmans, E.C., Pancost, R.D. & Damsté, J.S.S. (2000). Widespread occurrence of structurally diverse tetraether membrane lipids: Evidence for the ubiquitous presence of low-temperature relatives of hyperther-

mophiles. Proceedings of the National Academy of Sciences, 97(26), 14421. doi:10.1073/pnas.97.26.14421.

Schouten, S., Hopmans, E.C. & Sinninghe Damsté, J.S. (2013). The organic geochemistry of glycerol dialkyl glycerol tetraether lipids: A review. Organic Geochemistry, 54, 19-61. doi:10.1016/j.orggeochem.2012.09.006.

Schulz, M. & Mudelsee, M. (2002). REDFIT: estimating red-noise spectra directly from unevenly spaced paleoclimatic time series. Computers & Geosciences, 28(3), 421-426. doi:10.1016/S0098-3004(01)00044-9.

Steinhilber, F., Abreu, J.A., Beer, J., Brunner, I., Christl, M., Fischer, H., et al. (2012). 9,400 years of cosmic radiation and solar activity from ice cores and tree rings. Proceedings of the National Academy of Sciences, 109(16), 5967. doi:10.1073/pnas.1118965109.

Struve, T., Wilson, D.J., van de Flierdt, T., Pratt, N. & Crocket, K.C. (2020). Middle Holocene expansion of Pacific Deep Water into the Southern Ocean. Proceedings of the National Academy of Sciences, 117(2), 889. doi:10.1073/pnas.1908138117.

Stuiver, M., Reimer, P.J., Bard, E., Beck, J.W., Burr, G.S., Hughen, K.A., et al. (1998). INTCAL98 Radiocarbon Age Calibration, 24,000–0 cal BP. Radiocarbon, 40(3), 1041-1083. doi:10.1017/S0033822200019123.

Sun, Q., Chu, G., Liu, M., Xie, M., Li, S., Ling, Y., et al. (2011). Distributions and temperature dependence of branched glycerol dialkyl glycerol tetraethers in recent lacustrine sediments from China and Nepal. Journal of Geophysical Research, 116(G1). doi:10.1029/2010jg001365.

Tian, L., Wang, M., Zhang, X., Yang, X., Zong, Y., Jia, G., et al. (2019). Synchronous change of temperature and moisture over the past 50 ka in subtropical southwest China as indicated by biomarker records in a crater lake. Quaternary Science Reviews, 212, 121-134. doi:10.1016/j.quascirev.2019.04.003.

Tierney J.E. & deMenocal Peter, B. (2013). Abrupt Shifts in Horn of Africa Hydroclimate Since the Last Glacial Maximum. Science, 342(6160), 843-846. doi:10.1126/science.1240411.

Tierney, J.E. & Russell, J.M. (2009). Distributions of branched GDGTs in a tropical lake system: Implications for lacustrine application of the MBT/CBT paleoproxy. Organic Geochemistry, 40(9), 1032-1036. doi:10.1016/j.orggeochem.2009.04.014.

Tierney, J.E., Russell, J.M., Eggermont, H., Hopmans, E.C., Verschuren, D. & Sinninghe Damsté, J.S. (2010). Environmental controls on branched tetraether lipid distributions in tropical East African lake sediments. Geochim. Cosmochim. Acta, 74(17), 4902-4918. doi:10.1016/j.gca.2010.06.002.

Vinther, B.M., Clausen, H.B., Johnsen, S.J., Rasmussen, S.O., Andersen, K.K., Buchardt, S.L., et al. (2006). A synchronized dating of three Greenland ice

cores throughout the Holocene. Journal of Geophysical Research: Atmospheres, 111(D13). doi:10.1029/2005JD006921.

Wang, L., Li, J., Lu, H., Gu, Z., Rioual, P., Hao, Q., et al. (2012). The East Asian winter monsoon over the last 15,000 years: its links to high-latitudes and tropical climate systems and complex correlation to the summer monsoon. Quaternary Science Reviews, 32, 131-142. doi:10.1016/j.quascirev.2011.11.003.

Wang, X., Chu, G., Sheng, M., Zhang, S., Li, J., Chen, Y., et al. (2016). Millennial-scale Asian summer monsoon variations in South China since the last deglaciation. Earth and Planetary Science Letters, 451, 22-30. doi:10.1016/j.epsl.2016.07.006.

Wang, Z., Zhang, W. & Geng, X. (2017). Temporal and spatial variations of the first and last frost dates in China's inland agricultural region from 1961to 2014and their relationships with circulation factors. Acta Meteorologica Sinica, 75(4), 564-580.

Weijers, J.W.H., Schouten, S., van den Donker, J.C., Hopmans, E.C. & Damste, J.S.S. (2007). Environmental controls on bacterial tetraether membrane lipid distribution in soils. Geochim. Cosmochim. Acta, 71(3), 703-713. doi:10.1016/j.gca.2006.10.003.

Yancheva, G., Nowaczyk, N.R., Mingram, J., Dulski, P., Schettler, G., Negendank, J.F.W., et al. (2007). Influence of the intertropical convergence zone on the East Asian monsoon. Nature, 445(7123), 74-77. doi:10.1038/nature05431.

Yang, H., Pancost, R.D., Dang, X., Zhou, X., Evershed, R.P., Xiao, G., et al. (2014). Correlations between microbial tetraether lipids and environmental variables in Chinese soils: Optimizing the paleo-reconstructions in semi-arid and arid regions. Geochim. Cosmochim. Acta, 126, 49-69. doi:10.1016/j.gca.2013.10.041.

Yuan, D., Cheng, H., Edwards, R.L., Dykoski, C.A., Kelly, M.J., Zhang, M., et al. (2004). Timing, Duration, and Transitions of the Last Interglacial Asian Monsoon. Science, 304(5670), 575-578. doi:10.1126/science.1091220.

Zink, K.G., Vandergoes, M.J., Bauersachs, T., Newnham, R.M., Rees, A.B.H. & Schwark, L. (2016). A refined paleotemperature calibration for New Zealand limnic environments using differentiation of branched glycerol dialkyl glycerol tetraether (brGDGT) sources. Journal of Quaternary Science, 31(7), 823-835. doi:10.1002/jqs.2908.